nature cell biology

SPEECHLESS integrates brassinosteroid and stomata signalling pathways

Gustavo E. Gudesblat[1,2,5], Joanna Schneider-Pizoń[1,2,6], Camilla Betti[1,2,6], Juliane Mayerhofer[3,6], Isabelle Vanhoutte[1,2], Walter van Dongen[4], Sjef Boeren[4], Miroslava Zhiponova[1,2,5], Sacco de Vries[4], Claudia Jonak[3] and Eugenia Russinova[1,2,7]

Stomatal formation is regulated by multiple developmental and environmental signals, but how these signals are integrated to control this process is not fully understood[1]. In *Arabidopsis thaliana*, the basic helix-loop-helix transcription factor SPEECHLESS (SPCH) regulates the entry, amplifying and spacing divisions that occur during stomatal lineage development. SPCH activity is negatively regulated by mitogen-activated protein kinase (MAPK)-mediated phosphorylation[2]. Here, we show that in addition to MAPKs, SPCH activity is also modulated by brassinosteroid (BR) signalling. The GSK3/SHAGGY-like kinase BR-INSENSITIVE2 (BIN2) phosphorylates residues overlapping those targeted by the MAPKs, as well as four residues in the amino-terminal region of the protein outside the MAPK target domain. These phosphorylation events antagonize SPCH activity and limit epidermal cell proliferation. Conversely, inhibition of BIN2 activity *in vivo* stabilizes SPCH and triggers excessive stomata and non-stomatal cell formation. We demonstrate that through phosphorylation inputs from both MAPKs and BIN2, SPCH serves as an integration node for stomata and BR signalling pathways to control stomatal development in *Arabidopsis*.

Stomatal lineage in *Arabidopsis thaliana* is initiated by asymmetric divisions of undifferentiated meristemoid mother cells, to generate meristemoids and larger stomatal lineage ground cells (SLGCs). Meristemoids either differentiate into guard mother cells that divide symmetrically and form stomata, or undergo several amplifying divisions to produce more SLGCs. The SLGCs give rise to pavement cells and new satellite meristemoids through asymmetric spacing divisions[1,3,4]. All of these divisions require the basic helix-loop-helix (bHLH) transcription factor SPEECHLESS (ref. 5), whereas the transition from meristemoid to guard mother cell and its subsequent symmetric divisions involve the closely related bHLHs, MUTE and FAMA (refs 5–7). The activity of SPCH, MUTE and FAMA is regulated by a repressive signalling cascade, initiated from the cell surface by direct binding of extracellular peptides, that belong to the EPIDERMAL PATTERNING FACTOR (EPF) family of the leucine-rich repeat (LRR) receptor-like kinases of the ERECTA (ER) family of which the activity is modulated by the LRR receptor-like protein TOO MANY MOUTHS[8] (TMM). These receptors are genetically upstream of a canonical MAPK signalling module, involving YODA (YDA), MKK4/MKK5 and MPK3/MPK6, the activation of which results in SPCH phosphorylation and inactivation[2,9–11].

Despite the advances in the understanding of the mechanisms that control stomatal development[1,3–8], the modulation of this pathway by environmental and endogenous developmental signals, including plant hormones, remains unknown. BRs are hormones that affect many aspects of plant development by promoting cell expansion and cell division[12–15]. BRs act through a BR-INSENSITIVE1 (BRI1) receptor-mediated signal transduction pathway that inactivates the serine/threonine glycogen synthase kinase 3 (GSK3)/SHAGGY-like BR-INSENSITIVE2 (BIN2) kinase and induce the dephosphorylation of two key transcription factors BRASSINAZOLE RESISTANT1 (BZR1) and *bri1*-EMS-SUPPRESSOR1 (BES1)/BZR2, resulting in BR responses[16].

To better understand the role of BRs in plant development, we studied the epidermis of *Arabidopsis* mutants *constitutive photomorphogenesis and dwarfism* (*cpd*; ref. 17) that is unable to synthesize BRs and *bri1-116* that is affected in BR perception[18]. Microscopic observations revealed that in both mutants the number of stomata in the hypocotyls was strongly reduced (Fig. 1a,b and Supplementary Fig. S1a) and the stomatal index (number of stomata per total epidermal

[1]Department of Plant Systems Biology, VIB, 9052 Gent, Belgium. [2]Department of Plant Biotechnology and Bioinformatics, Ghent University, 9052 Gent, Belgium. [3]GMI–Gregor Mendel Institute of Molecular Plant Biology, Austrian Academy of Sciences, 1030 Vienna, Austria. [4]Laboratory of Biochemistry, Wageningen University, 6703 HA Wageningen, The Netherlands. [5]Present addresses: Instituto de Ciencia y Tecnología 'Dr. Cesar Milstein', Fundación Pablo Cassará, Consejo Nacional de Investigaciones Científicas y Técnicas, C1440FFX, Buenos Aires, Argentina (G.E.G.); Faculty of Biology, Department of Plant Physiology, University of Sofia, 1164 Sofia, Bulgaria (M.Z.). [6]These authors contributed equally to this work.
[7]Correspondence should be addressed to E.R. (e-mail: jenny.russinova@psb.vib-ugent.be)

Received 1 June 2011; accepted 28 February 2012; published online XX Month XXXX; DOI: 10.1038/ncb2471

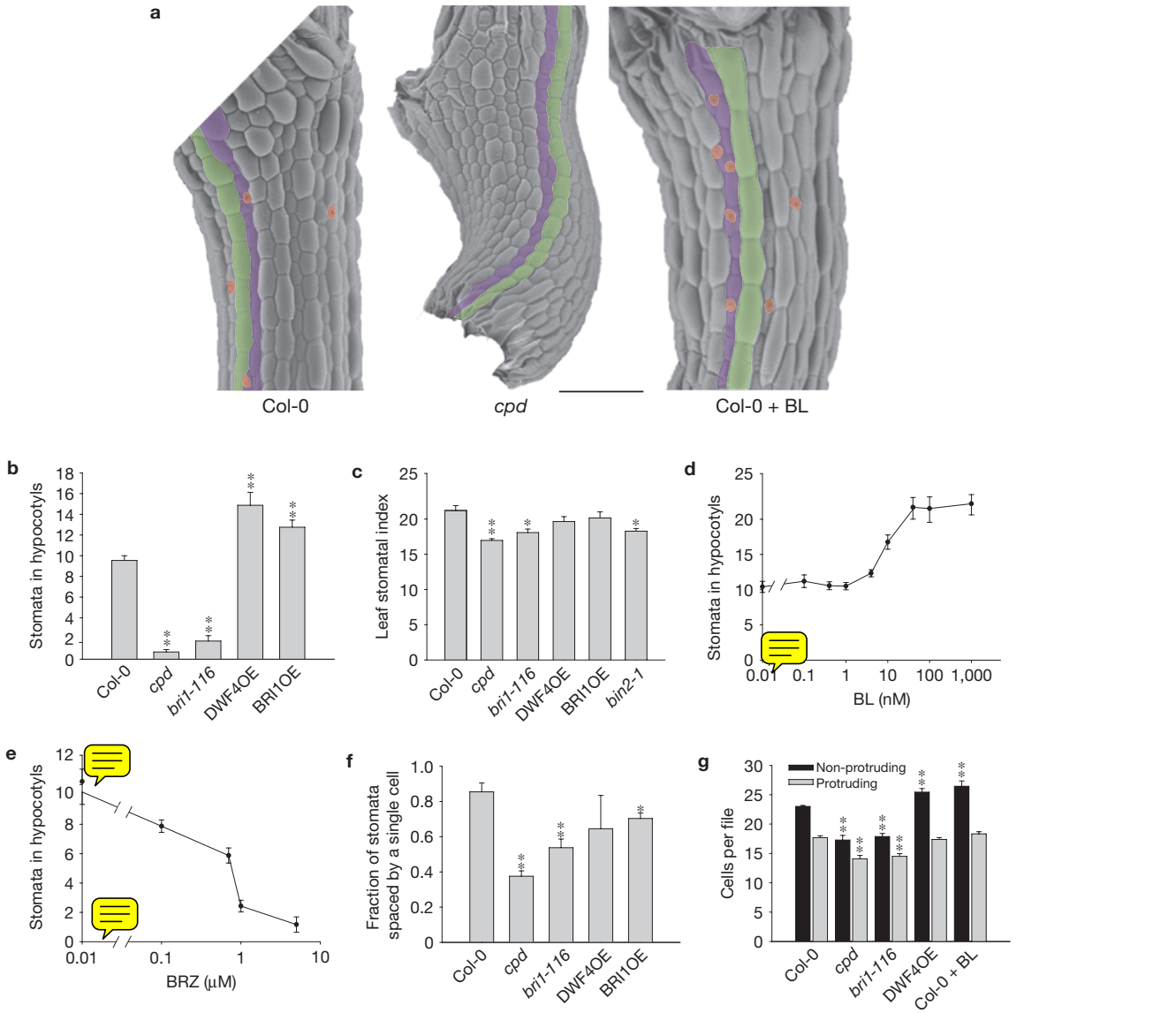

Figure 1 BRs control stomatal development. (**a**) Scanning electron micrographs of 8-day-old hypocotyls of the indicated genotypes. The wild-type Col-0 plant was treated with 10 nM BL. Protruding, non-protruding cell files and stomata are coloured in green, purple and red, respectively. Scale bar, 100 μm. (**b**) Overexpression of *DWF4* and *BRI1* increases the total number of stomata in hypocotyls, whereas *cpd* and *bri1-116* mutations reduce it ($n = 8$). (**c**) *cpd*, *bri1-116* and *bin2-1* mutations, but not *DWF4* and *BRI1* overexpression, significantly reduce the leaf stomatal index of 21-day-old plants ($n = 6$). (**d**,**e**) Dose-response curves for the effect of BL and BRZ on stomatal development in the hypocotyl ($n = 8$). (**f**) A decrease in the endogenous levels or perception of BRs, or increased *BRI1* receptor gene expression, reduces the fraction of stomata spaced by one single cell in 21-day-old leaves ($n = 8$). (**g**) In Col-0 plants, 10 nM BL significantly increases non-stomatal cells in non-protruding cell files. This number is also increased in DWF4OE and decreased in *cpd* and *bri1-116*, whereas the number of non-stomatal cells in protruding files of these two mutants is also reduced ($n = 10$). Error bars indicate s.e.m. *P* values (*t*-test), * < 0.05 and ** < 0.01 re to the respective control. *n*, number of leaves (**c**,**f**) or seedlings (**a**,**d**, **e**,**g**) analysed.

cells) of leaves, but not of cotyledons was slightly decreased (Fig. 1c and Supplementary Fig. S1b,c). Conversely, in transgenic plants with enhanced BR responses due to overexpression of either the BR biosynthesis gene *DWARF4* (*DWF4*; DWF4OE; ref. 19) or the BR receptor BRI1 (BRI1OE; ref. 18), the number of stomata increased significantly in hypocotyls (Fig. 1b and Supplementary Fig. S1a) and the stomatal index only in cotyledons of BRI1OE plants (Supplementary Fig. S1c). Close observation of the leaf epidermis of *bri1-116* and *cpd* revealed a decrease in the fraction of stomata separated by a single cell, a parameter potentially indicative of defects in spacing divisions[5] (Fig. 1f and Supplementary Fig. S1b). Interestingly, BRI1OE also showed a small reduction in this fraction (Fig. 1f and Supplementary Fig. S1b), indicating that a precise amount of BRI1 receptors is required to achieve the epidermal patterning observed in wild-type plants. In agreement with the phenotypes observed in BR mutants and transgenic *Arabidopsis* plants, treatment with 4 nM of the most active BR hormone, brassinolide (BL), was sufficient to trigger an increase in the number of stomata in hypocotyls, whereas no further increase was observed at concentrations above 40 nM (Fig. 1a,d and Supplementary Fig. S1d). In contrast, concentrations of 0.1 μM and higher of the BR biosynthesis

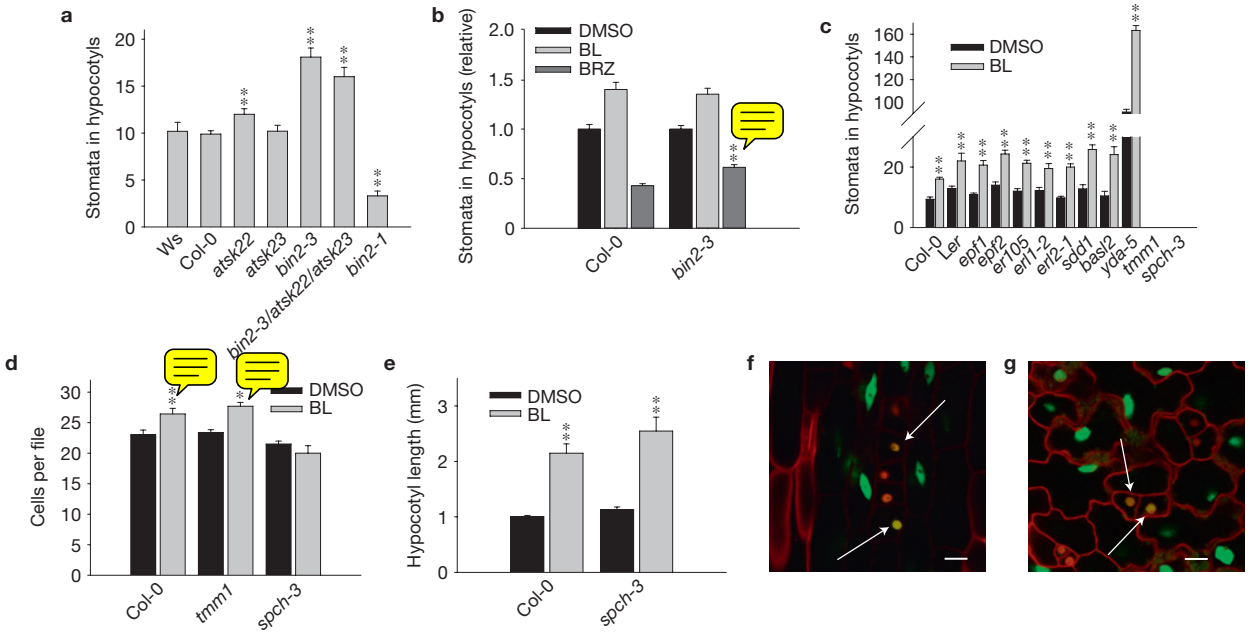

Figure 2 SPCH is required for the effect of BRs on stomatal development and epidermal cell division in the hypocotyl. (**a**) *bin2-3*, *atsk22* and *bin2-3/atsk22/atsk23* have an increased number of stomata in hypocotyls relative to the controls, whereas this number is reduced in the *bin2-1* mutant ($n = 8$). (**b**) *bin2-3* mutants are partially resistant to 1 μM BRZ but not to 10 nM BL for the number of stomata in hypocotyls ($n = 8$). [illegible]eatment with 10 nM BL promotes stomata development in Col-0, L*er*, *epf1*, *epf2*, *er-105*, *erl1-2*, *erl2-1*, *sdd1*, *basl2* and *yda-5*, but not in *tmm* or *spch-3* ($n = 8$). (**d**) 10 nM BL significantly increases the number of non-stomatal cells in non-protruding files in Col-0 and *tmm*, but not in *spch-3* ($n = 15$). (**e**) *spch-3* responds to 10 nM BL as Col-0 f[illegible]ocotyl elongation ($n = 6$). Error bars indicate s.e.m. *P* values (*t*-test), * < 0.05 and ** < 0.01 relative to the DMSO (**b**–**e**) and Ws (**a**) controls. *n*, number of seedlings analysed. (**f**,**g**) *SPCHprom::nRFP* and *BIN2prom::nGFP* reporters are co-expressed in small cells in non-protruding cell files in hypocotyl epidermis (**f**) and in small cells of the abaxial cotyledon epidermis (**g**). The arrows point to yellow nuclei from 2.5-day-old seedlings counterstained with propidium iodide. Scale bars, 10 μm.

inhibitor brassinazole[20] (BRZ) significantly reduced the number of stomata in hypocotyls (Fig. 1e and Supplementary Fig. S1e).

BRs control cell fate specification in the root epidermis through the control of the expression of the transcription factors *WEREWOLF* and *GLABRA2* (ref. 21), also known to specify cell fate in the hypocotyl epidermis as mutations in these genes cause ectopic stomata production in protruding cell files of hypocotyls[22]. Therefore, we investigated whether BRs also affect cell fate specification in this organ. Notably, the excess of BRs not only enhanced the number of stomata, but also the cell divisions (a prerequisite for stomatal development in hypocotyls[23]) limited exclusively to non-protruding cell files (Fig. 1a and Supplementary Fig. S1f). In contrast, *bri1-116* and *cpd* mutations caused a reduction in the number of cell divisions in both non-protruding and protruding cell files (Fig. 1g). Together, these results show that BRs promote epidermal cell divisions and stomatal development in hypocotyls without affecting the cell fate.

Consistent with reports that the group II GSK3/SHAGGY-like kinases of *Arabidopsis* BIN2, ATSK22 and ATSK23 play redundant roles as negative regulators in BR signalling[24,25], the triple knockout *bin2-3/atsk22/atsk23* (ref. 24) and the single *bin2-3* mutants showed a similar increase in the number of stomata in hypocotyls (Fig. 2a), implying a major role for BIN2 in mediating the effect of BRs on stomatal development. Although the stomata numbers of hypocotyls in the *bin2-3* mutant were less affected by BRZ, its BL sensitivity was not changed (Fig. 2b), indicating that other *Arabidopsis* GSK3/SHAGGY-like kinases might act redundantly with BIN2 in the control of stomatal development. The stomatal index of *bin2-3* or *bin2-3/atsk22/atsk23* leaves was not affected (Supplementary Fig. S2a). In contrast, the gain-of-function *bin2-1* mutant, incapable of responding to BRs (Supplementary Fig. S2b) owing to enhanced BIN2 activity[26], exhibited a strongly reduced number [illegible]omata in hypocotyls (Fig. 2a), as well as decreased Supplementary Information in leaves (Fig. 1c). Unlike the number of stomata in hypocotyls, the length of this organ in *bin2-3* was similar to that of wild-type plants (Supplementary Fig. S2c), indicating that the effect of BRs on stomatal development is uncoupled from its effect on cell elongation. Contrary to the *bin2-3* mutant, the gain-of-function mutants *bes1-D* (ref. 27) and *bzr1-D* (ref. 28), affected in genes encoding the known phosphorylation targets of BIN2, BZR1 and BZR2/BES1, had a normal number of stomata in hypocotyls (Supplementary Fig. S2d). Therefore, we conclude that BIN2 negatively regulates stomatal development by phosphorylation of downstream targets different from BZR1 or BZR2/BES1.

As a result of the clear effect of BRs on stomatal formation in hypocotyls, we studied the response to BL in mutants affected in stomatal development in this organ. BRs increased the number of stomata in hypocotyls of mutants affected in the stomatal receptor–ligand complex, *epf1* (ref. 29), *epf2* (refs 30,31), *er-105*, *erl1-2* and *erl2-1* (ref. 32), in the negative regulator of stomatal formation stomatal density and distribution1 (SDD1), *sdd1* (ref. 33), in the stomata polarity determinant breaking of asymmetry in the stomatal lineage (BASL), *basl2* (ref. 34), and in the MAPK kinase kinase YODA, *yda-5* (ref. 10; Fig. 2c), indicating that the BRs act downstream or independently from the genes affected in these mutants. Remarkably, BL failed to promote stomatal development in hypocotyls of *tmm*

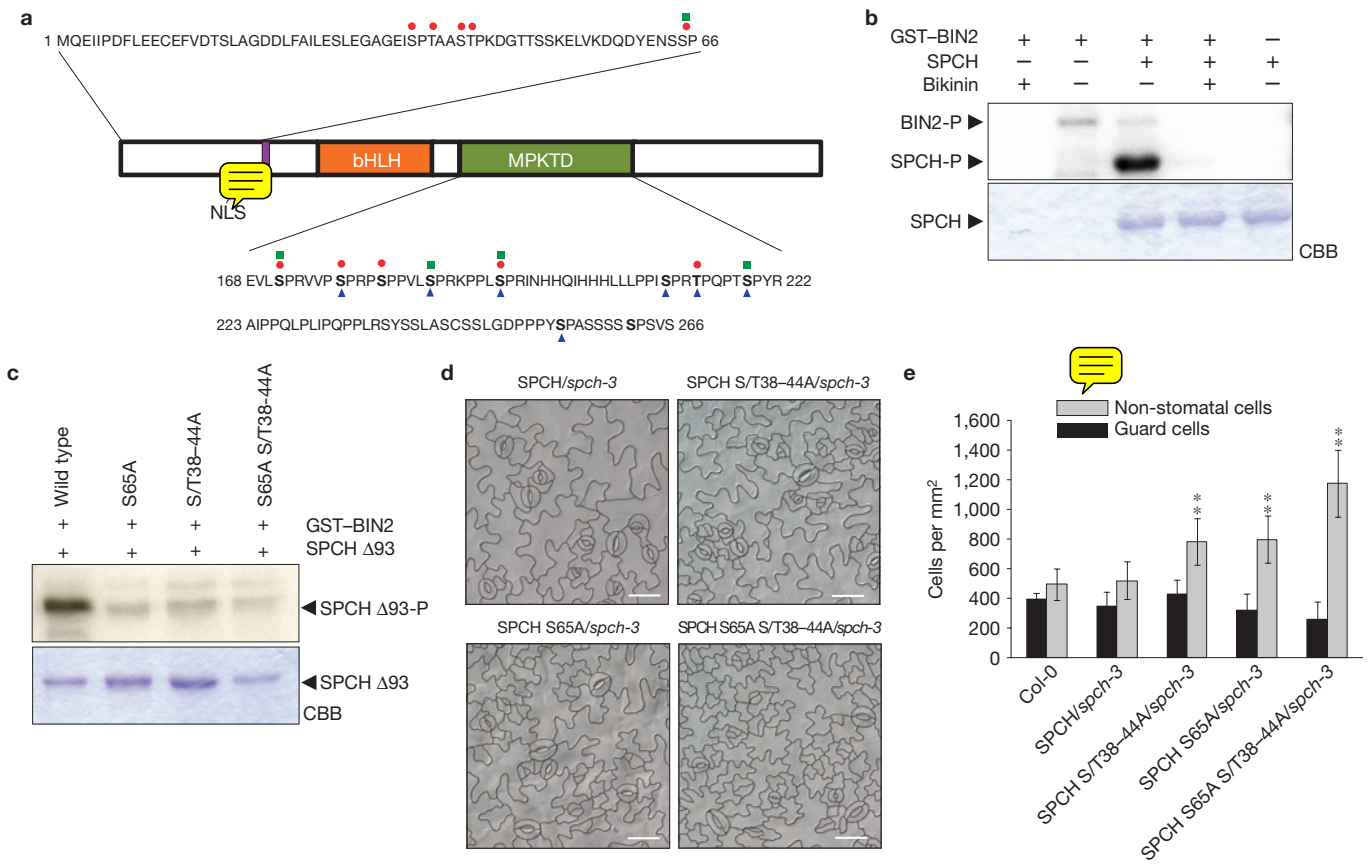

Figure 3 BIN2 phosphorylates SPCH. (**a**) Scheme of the SPCH protein indicating BIN2 phosphorylation sites. The red dots mark *in vitro* BIN2 phosphorylation targets (this study), blue triangles previously described MAPK *in vitro* phosphorylation targets[2] and green squares residues found to be phosphorylated *in vivo* (this study). Residues in bold are predicted MAPK phosphorylation targets[2]. (**b**) Phosphorylation of SPCH (relative molecular mass, 40,000 (M_r 40K)) by GST–BIN2 *in vitro*. Kinase assays were performed with purified GST–BIN2 and SPCH in the presence or absence of 10 μM of the BIN2-specific kinase inhibitor bikinin[37]. The top band observed in the second and third lanes corresponds to the autophosphorylated GST–BIN2 (M_r 68K). (**c**) SPCH deleted for the MPKTD (GST–SPCHΔ93) (M_r 35K) is phosphorylated by GST–BIN2, whereas substitutions S65A or S/T38–44A in combination with Δ93 diminish its phosphorylation. CBB, Coomassie brilliant blue gel staining (loading controls). Full scans of the blot and gel in **c** are shown in Supplementary Fig. S6. (**d**,**e**) Abaxial epidermis of 8-day-old cotyledons of *spch-3* mutants complemented with *SPCHprom::SPCH, SPCHprom::SPCH S65A, SPCHprom::SPCH S/T38–44A* and *SPCHprom::SPCH S65A S/T38–44A* exhibit increased non-stomatal cell density ($n = 8$). Error bars indicate s.e.m. P values (t-test), ** < 0.01 relative to the non-stomatal cells of the *SPCHprom::SPCH* line. Scale bars, 20 μm. n, number of seedlings analysed.

(ref. 35) and *spch-3* (ref. 5) mutants. Both TMM and SPCH are required for stomatal formation in hypocotyls, but whereas in *spch-3* mutants asymmetric divisions do not occur[5], in *tmm* hypocotyls stomatal development arrests after a SPCH-dependent asymmetric division[36], implying that cell divisions preceding meristemoid mother cell asymmetric divisions take place in this mutant[23]. BL treatment of hypocotyls of these mutants led to BR-induced cell proliferation in non-protruding files of *tmm*, but not of *spch-3* (Fig. 2d), confirming that SPCH, but not TMM, is required for the promotive effect of BRs on stomatal development. In contrast, the BL sensitivity of *spch-3* on hypocotyl elongation was not affected (Fig. 2e). Consistent with the possible role of SPCH in mediating the effect of BRs in stomatal development, in plants co-expressing the transcriptional reporters *SPCHprom::nRFP* and *BIN2prom::nGFP* overlapping expression was observed in small cells of non-protruding hypocotyl cell files (Fig. 2f) and of developing cotyledon epidermis (Fig. 2g).

Next, we investigated whether BIN2 directly controls SPCH activity by phosphorylation. GST–BIN2 phosphorylated SPCH *in vitro* (Fig. 3b) and this effect was abolished after incubation with the BIN2-specific inhibitor bikinin[37]. Mass spectrometry analysis identified *in vitro* phosphorylation in SPCH by BIN2 on residues Ser 171, Ser 177, Ser 181, Ser 193 and Thr 214 located within the 93-amino-acid MAPK target domain (MPKTD)[2], all of which, except Ser 171 and Ser 181, have been reported previously as MAPK targets[2]. Additional phosphorylation of SPCH by BIN2 was found in residues Ser 65, Ser 38, Thr 40, Ser 43 and Thr 44 located at the N-terminal part of the protein and outside the MPKTD (Fig. 3a and Supplementary Table S1). The ability of BIN2 to target residues outside the MPKTD was confirmed by its capacity to phosphorylate SPCH lacking this domain (SPCHΔ93; Fig. 3c and Supplementary Fig. S2e) that was not phosphorylated by MPK3 or MPK6 (ref. 2). To verify that BIN2 targets residues outside the MPKTD of SPCH, we replaced Ser 65, Ser 38, Thr 40, Ser 43 and Thr 44 in SPCHΔ93 with alanine to prevent phosphorylation, resulting in the mutant combinations S65A, S/T38–44A and S65A S/T38–44A. The substitutions S65A and S/T38–44A, as well as their combination, markedly reduced the phosphorylation of SPCHΔ93 by BIN2 (Fig. 3c), confirming that these residues are BIN2 targets. Furthermore, the evolutionarily conserved Ser 65 (Supplementary Fig.

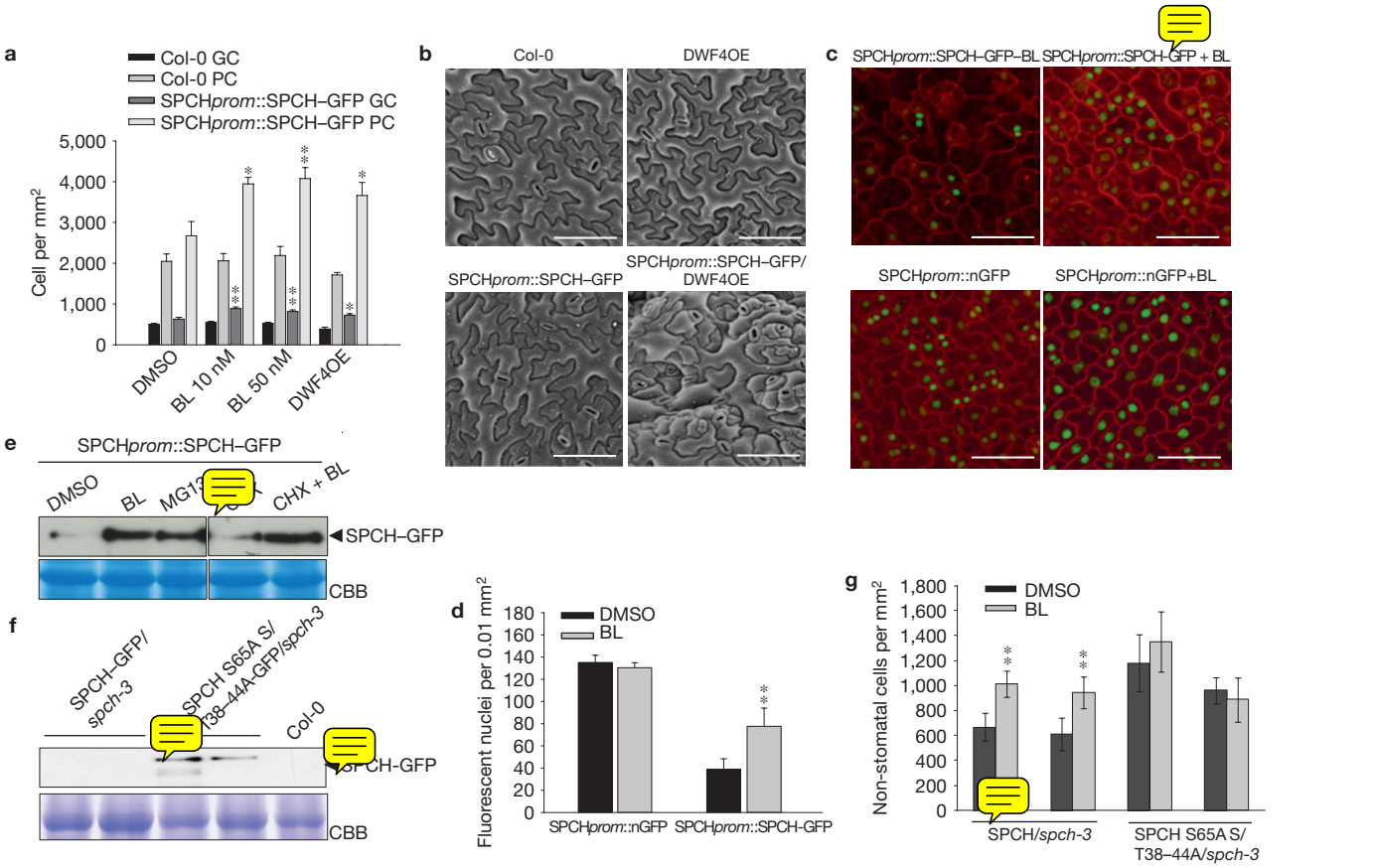

Figure 4 Effect of BRs on stomatal development in leaves and cotyledons. (**a**) Treatment with 10 nM and 50 nM BL significantly increases the pavement and guard cell densities of 4-day-old cotyledons from Col-0 plants expressing *SPCHprom::SPCH–GFP* (refs 2,5), but not in the control ($n = 8$). GC, guard cells; PC, pavement cells. The same effect was observed after crossing the *SPCHprom::SPCH–GFP*-expressing line[2,5] into a DWF4OE background. DWF4OE had reduced pavement cell and guard cell densities relative to the wild type as a result of increased cell expansion. (**b**) Overexpression of *DWF4* increases the stomatal and pavement cell densities in abaxial epidermis of 21-day-old leaves expressing the reporter *SPCHprom::SPCH–GFP* (refs 2,5), but not of an otherwise wild-type background. Scale bars, 30 μm. (**c**,**d**) Abaxial epidermis of cotyledons from 2.5-day-old seedlings grown in 10 nM BL shows an increased number of *GFP*-expressing nuclei when carrying the translational *SPCHprom::SPCH–GFP* (refs 2,5), but not the transcriptional *SPCHprom::nGFP* (ref. 5) reporter ($n = 10$). Scale bars, 10 μm. (**e**) Treatment of 2.5-day-old seedlings expressing *SPCHprom::SPCH–GFP* (refs 2,5) with 50 nM BL, 100 μM MG132, 100 μM cycloheximide (CHX) or 50 nM BL together with 100 μM cycloheximide for 2 h. The amount of immunoprecipitated SPCH–GFP (M_r 75K) proteins was examined by western blotting with an anti-GFP antibody. (**f**) Immunoprecipitation and detection of SPCH–GFP as in **e** from 2.5-day-old *spch-3* mutant seedlings complemented with GFP-tagged *SPCHprom::SPCH S65A S/T38–44A* and *SPCHprom::SPCH* constructs. Two independent transgenic lines for each construct are shown. Confirmation of the presence of SPCH–GFP protein in complemented *spch-3* is shown in Supplementary Fig. S4e. CBB, Coomasie brilliant blue gel staining (loading control). Fu[illegible]s of the blot and gel in **e**, **f** are shown in Supplementary Fig. S6. (**g**) [illegible]eatment with 10 nM BL increases the number of non-stomatal cells in cotyledons of the *spch-3* mutant complemented with the *SPCHprom::SPCH* but not in *spch-3* plants expressing the *SPCHprom::SPCH S65A S/T38–44A* construct ($n = 8$). Error bars indicate s.e.m. *P* values (*t*-test), * < 0.05 and ** < 0.01 relative to the respective DMSO controls. *n*, number of cotyledons analysed.

S2f) and the MPKTD residues Ser 171, Ser 186, Ser 193 and Ser 219 were phosphorylated *in vivo* in *Arabidopsis* seedlings expressing the *SPCHprom::SPCH–GFP* construct[2,5] (Fig. 3a and Supplementary Table S2A). Mass spectrometry analyses after BL treatment revealed an absence of phosphorylation in Ser 65 and an approximately fivefold reduction in Ser 171 and Ser 186 phosphorylated residues (Supplementary Table S2B and Fig. S3a). This, together with the increased production of the SPCH–GFP protein on BL treatment (Supplementary Fig. S4b), indicates that dephosphorylation of SPCH Ser 65, Ser 171 and Ser 186 residues *in planta* is under strict control of BRs.

The functional relevance of the BIN2-specific phosphorylation of SPCH was evaluated by introducing the *SPCHprom::SPCH S65A*, *SPCHprom::SPCH S/T38–44A* and *SPCHprom::SPCH S65A S/T38–44A* constructs into the *spch-3* mutant. All mutant versions of SPCH rescued the production of stomata in the *spch-3* epidermis similarly as in the wild-type protein. Remarkably, in the three constructs expressing the mutated SPCH the number of non-stomatal epidermal cells increased significantly (Fig. 3d,e and Supplementary Fig. S3b,c). This effect was more pronounced in lines expressing the *SPCH S65A S/T38–44A* variant, indicating that the joint BIN2-dependent phosphorylation is required in these sites to limit proliferation of non-stomatal epidermal cells by SPCH, similar to some of the MPKTD phosphorylation targets[2].

An increase in *SPCH* expression within its native domain considerably enhanced stomatal phenotypes in cotyledons of *tmm* or *erl1/erl2* double mutants[2,5] presumably due to increased MPK3 and MPK6 activities. Therefore, we reasoned that reducing the BIN2 activity by increasing BR levels in plants expressing *SPCHprom::SPCH–GFP* (refs 2,5) would also promote stomata accumulation in cotyledons, which might not occur in wild-type plants because of the redundant action of MAPKs. Accordingly, BL treatment of *SPCHprom::SPCH–GFP*-expressing plants[2,5] and introduction of the *SPCHprom::SPCH–GFP* construct[2,5] into a DWF4OE background resulted in a significant

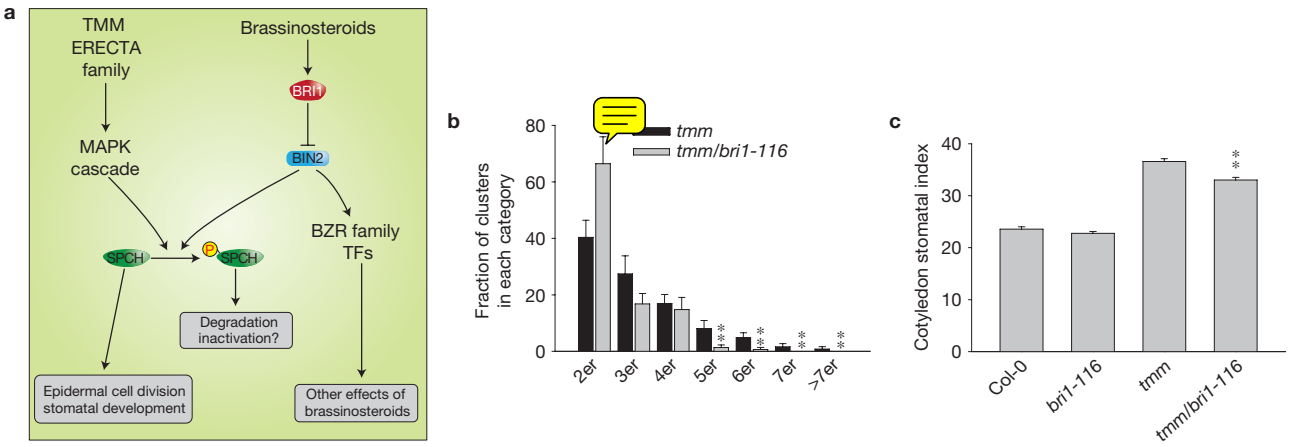

Figure 5 BRs and the MAPK signalling pathways concertedly control SPCH activity to regulate stomatal development. (**a**) Model of action of BRs on stomatal development. BRs bind to the BRI1 membrane receptor, thereby triggering BIN2 inactivation. When active, BIN2 phosphorylates and thus inactivates and/or targets for degradation the transcription factor SPCH that is required for the asymmetric cell division involved in meristemoid formation. The MAPK signalling cascade, genetically downstream of the ERECTA family and TMM receptors, and the BR-regulated BIN2 signalling pathway act in coordination to regulate SPCH activity. (**b**,**c**) *bri1-116* mutation reduces the stomatal index ($n =$) and cluster complexity ($n = 10$; **c**) of *tmm* in 8-day-old cotyledons. Error bars indicate s.e.m. *P* values (*t*-test), ** < 0.01. *n*, number of cotyledons analysed.

increase of both stomata and pavement cell numbers in leaves and cotyledons (Fig. 4a,b and Supplementary Fig. S4a). The promotive effect of BRs on epidermal cell division and stomatal development in 2.5-day-old seedlings expressing *SPCHprom::SPCH–GFP* correlated with the SPCH accumulation in the presence of high concentrations of endogenous or exogenous BL and SPCH reduction in the presence of BRZ (Supplementary Fig. S4b). Correspondingly, under the same conditions seedlings expressing the translational reporter *SPCHprom::SPCH–GFP* (refs 2,5), but not the transcriptional reporter *SPCHprom::nGFP* (ref. 5), showed an increase in the number of fluorescent nuclei in response to BL (Fig. 4c,d), indicating that BRs promote epidermal cell division and stomata development by regulating the SPCH abundance post-translationally. In agreement, short BL treatments of wild-type and *SPCHprom::SPCH–GFP*-expressing plants[2,5] induced a several-fold increase in the amount of the SPCH protein (Fig. 4e), but did not cause a substantial increase in *SPCH* gene expression (Supplementary Fig. S4c). Further proof of the post-translational action of BRs on SPCH came from the lack of an effect of the protein synthesis inhibitor cycloheximide on the short-term BL-induced SPCH protein accumulation, whereas treatment with the proteasome inhibitor MG132 effectively increased the amount of SPCH protein (Fig. 4e). Consistent with our hypothesis that BIN2 controls the SPCH activity through direct phosphorylation, in the *spch-3* mutant complemented with the GFP-tagged SPCH protein carrying alanine substitutions in all BIN2-specific phosphorylation sites (S65A and S/T38–44A) the SPCH protein increased (Fig. 4f and Supplementary Fig. S4d,e). In agreement with these results, the *spch-3* mutant complemented with the *SPCHprom::SPCH* construct exhibited an increase in non-stomatal cells of the cotyledon epidermis after BL treatment, which was not observed in *spch-3* expressing SPCH protein containing the S65A and S/T38–44A substitutions (Fig. 4g). Thus, the effect of BRs on SPCH activity is mediated, at least in part, by BIN2 phosphorylation of these residues.

Our results indicate that BRs regulate epidermal and stomatal development by inhibition of BIN2 phosphorylation of SPCH (Fig. 5a) possibly in the nucleus where both proteins co-localize[5,24]. The less marked effects of BRs on stomatal development in cotyledons and leaves relative to hypocotyls are probably due to a redundant control of SPCH by BIN2 and MPK3/MPK6, which, for unknown reasons, seems to be more prominent in the epidermis of the former organs. At the molecular level, this redundancy is illustrated by the overlapping phosphorylation sites for both types of kinase within the SPCH MPKTD. The redundant control of the SPCH activity by MAPKs and BR signalling is also demonstrated by a partial rescue of the excessive stomatal index and of stomata clustering of the *tmm* mutation in a *bri1-116* mutant background (Fig. 5b,c). Yet the ability of BIN2 to phosphorylate residues outside the MPKTD, and the fact that mutations in these residues lead to an increase in non-stomatal cell divisions, indicates that BRs can modulate SPCH functions that are not under MAPK control, possibly through inhibition of its degradation. The fact that the *bri1-116* mutation reduces the higher-order stomatal complex divisions and the fraction of stomata spaced by a single cell in *tmm* mutants indicates that BRs might specifically control SPCH activity in spacing divisions. Apart from BIN2, other GSK3/SHAGGY-like kinases[38,39] might act redundantly on SPCH, as implied by the lack of both BR sensitivity decrease for stomata numbers in hypocotyls and SPCH protein stabilization in the *bin2-3* mutant (Fig. 2b and Supplementary Fig. S4f). Recently, another study showed that in contrast to our data BRs inhibit stomatal formation by BIN2-mediated activation of YDA (ref. 40). The different interactions between MAPK and GSK3-mediated signalling pathways reflect the highly orchestrated regulation of stomatal developmental in response to complex developmental cues and environmental signals. □

METHODS

Methods and any associated references are available in the online version of the paper at www.nature.com/naturecellbiology

Note: Supplementary Information is available on the Nature Cell Biology website

ACKNOWLEDGEMENTS

We thank D. Bergmann, K. Torii, F. Sack, G. Vert, S. Mora-García, A. I. Caño-Delgado, H-Q. Yang and T. Kakimoto for providing materials; K. Mechtler and N. Li for help in mass spectrometry; E. Mylle for technical assistance; and M. De Cock, A. Bleys, G. Van Isterdael and K. Van Lierde for help in preparing the manuscript.

This work is supported by the Marie-Curie Initial Training Network 'BRAVISSIMO' (grant no. PITN-GA-2008-215118), the Research Foundation-Flanders (grant no. G.0065.08), the Agency for Innovation by Science and Technology (IWT, 'Strategisch Basisonderzoek' grant no. 60839), the Centre for BioSystems Genomics, Systeemgenomics project CBSG2012-AA6 (S.d.V.) and the Austrian Academy of Sciences (J.M. and C.J.). G.E.G. and M.Z. are indebted to the Belgian Science Policy Office (BELSPO) and the Agency for Innovation by Science and Technology for a postdoctoral fellowship, respectively. G.E.G. is a Career Investigator of the Consejo Nacional de Investigaciones Científicas y Técnicas.

AUTHOR CONTRIBUTIONS

G.E.G. and E.R. conceived the project and designed experiments. G.E.G., C.B. and I.V. performed microscopy experiments. G.E.G., J.S-P., C.B. and I.V. did DNA manipulations. J.S-P. expressed proteins in bacteria; J.S-P. and C.B performed SPCH immunoprecipitation experiments. M.Z. segregated and characterized the *bin2-3*, *atsk22* and *atsk23* mutants. C.J. and J.M. designed and performed *in vitro* phosphorylation assays and subsequent mass spectrometry analyses. J.S-P., S.B. W.v.D. and S.d.V. did *in vivo* mass spectrometry analysis. G.E.G. and E.R. wrote the manuscript and J.S-P., M.Z., S.d.V., C.B. and C.J. revised it.

COMPETING FINANCIAL INTERESTS

The authors declare no competing financial interests.

Published online at www.nature.com/naturecellbiology
Reprints and permissions information is available online at www.nature.com/reprints

1. Bergmann, D. C. & Sack, F. D. Stomatal development. *Annu. Rev. Plant Biol.* **58,** 163–181 (2007).
2. Lampard, G. R., MacAlister, C. A. & Bergmann, D. C. *Arabidopsis* stomatal initiation is controlled by MAPK-mediated regulation of the bHLH SPEECHLESS. *Science* **322,** 1113–1116 (2008).
3. Robinson, S. *et al.* Generation of spatial patterns through cell polarity switching. *Science* **333,** 1436–1440 (2011).
4. Pillitteri, L. J., Peterson, K. M., Horst, R. J. & Torii, K. U. Molecular profiling of stomatal meristemoids reveals new component of asymmetric cell division and commonalities among stem cell populations in *Arabidopsis*. *Plant Cell* **23,** 3260–3275 (2011).
5. MacAlister, C. A., Ohashi-Ito, K. & Bergmann, D. C. Transcription factor control of asymmetric cell divisions that establish the stomatal lineage. *Nature* **445,** 537–540 (2007).
6. Ohashi-Ito, K. & Bergmann, D. C. *Arabidopsis* FAMA controls the final proliferation/differentiation switch during stomatal development. *Plant Cell* **18,** 2493–2505 (2006).
7. Pillitteri, L. J., Sloan, D. B., Bogenschutz, N. L. & Torii, K. U. Termination of asymmetric cell division and differentiation of stomata. *Nature* **445,** 501–505 (2007).
8. Lee, J. S. *et al.* Direct interaction of ligand-receptor pairs specifying stomatal patterning. *Genes Dev.* **26,** 126–136 (2012).
9. Lampard, G. R., Lukowitz, W., Ellis, B. E. & Bergmann, D. C. Novel and expanded roles for MAPK signaling in *Arabidopsis* stomatal cell fate revealed by cell type-specific manipulations. *Plant Cell* **21,** 3506–3517 (2009).
10. Bergmann, D. C., Lukowitz, W. & Somerville, C. R. Stomatal development and pattern controlled by a MAPKK kinase. *Science* **304,** 1494–1497 (2004).
11. Wang, H., Ngwenyama, N., Liu, Y., Walker, J. C. & Zhang, S. Stomatal development and patterning are regulated by environmentally responsive mitogen-activated protein kinases in *Arabidopsis*. *Plant Cell* **19,** 63–73 (2007).
12. Gudesblat, G. E. & Russinova, E. Plants grow on brassinosteroids. *Curr. Opin. Plant Biol.* **14,** 530–537 (2011).
13. González-García, M. P. *et al.* Brassinosteroids control meristem size by promoting cell cycle progression in *Arabidopsis* roots. *Development* **138,** 849–859 (2011).
14. Gonzalez, N. *et al.* Increased leaf size: different means to an end. *Plant Physiol.* **153,** 1261–1279 (2010).
15. Hacham, Y. *et al.* Brassinosteroid perception in the epidermis controls root meristem size. *Development* **138,** 839–848 (2011).
16. Kim, T-W. & Wang, Z-Y. Brassinosteroid signal transduction from receptor kinases to transcription factors. *Annu. Rev. Plant Biol.* **61,** 681–704 (2010).
17. Szekeres, M. *et al.* Brassinosteroids rescue the deficiency of CYP90, a cytochrome P450, controlling cell elongation and de-etiolation in *Arabidopsis*. *Cell* **85,** 171–182 (1996).
18. Friedrichsen, D. M., Joazeiro, C. A. P., Li, J., Hunter, T. & Chory, J. Brassinosteroid-insensitive-1 is a ubiquitously expressed leucine-rich repeat receptor serine/threonine kinase. *Plant Physiol.* **123,** 1247–1256 (2000).
19. Wang, Z. Y., Seto, H., Fujioka, S., Yoshida, S. & Chory, J. BRI1 is a critical component of a plasma-membrane receptor for plant steroids. *Nature* **410,** 380–383 (2001).
20. Asami, T. *et al.* Characterization of brassinazole, a triazole-type brassinosteroid biosynthesis inhibitor. *Plant Physiol.* **123,** 93–100 (2000).
21. Kuppusamy, K. T., Chen, A. Y. & Nemhauser, J. L. Steroids are required for epidermal cell fate establishment in *Arabidopsis* roots. *Proc. Natl Acad. Sci. USA* **106,** 8073–8076 (2009).
22. Serna, L. Epidermal cell patterning and differentiation throughout the apical-basal axis of the seedling. *J. Exp. Bot.* **56,** 1983–1989 (2005).
23. Berger, F., Linstead, P., Dolan, L. & Haseloff, J. Stomata patterning on the hypocotyl of *Arabidopsis thaliana* is controlled by genes involved in the control of root epidermis patterning. *Dev. Biol.* **194,** 226–234 (1998).
24. Vert, G. & Chory, J. Downstream nuclear events in brassinosteroid signalling. *Nature* **441,** 96–100 (2006).
25. Yan, Z., Zhao, J., Peng, P., Chihara, R. K. & Li, J. BIN2 functions redundantly with other *Arabidopsis* GSK3-like kinases to regulate brassinosteroid signaling. *Plant Physiol.* **150,** 710–721 (2009).
26. Li, J. & Nam, K. H. Regulation of brassinosteroid signaling by a GSK3/SHAGGY-like kinase. *Science* **295,** 1299–1301 (2002).
27. Yin, Y. *et al.* BES1 accumulates in the nucleus in response to brassinosteroids to regulate gene expression and promote stem elongation. *Cell* **109,** 181–191 (2002).
28. Wang, Z-Y. *et al.* Nuclear-localized BZR1 mediates brassinosteroid-induced growth and feedback suppression of brassinosteroid biosynthesis. *Dev. Cell* **2,** 505–513 (2002).
29. Hara, K., Kajita, R., Torii, K. U., Bergmann, D. C. & Kakimoto, T. The secretory peptide gene EPF1 enforces the stomatal one-cell-spacing rule. *Genes Dev.* **21,** 1720–1725 (2007).
30. Hunt, L. & Gray, J. E. The signaling peptide EPF2 controls asymmetric cell divisions during stomatal development. *Curr. Biol.* **19,** 864–869 (2009).
31. Hara, K. *et al.* Epidermal cell density is autoregulated via a secretory peptide, EPIDERMAL PATTERNING FACTOR 2 in *Arabidopsis* leaves. *Plant Cell Physiol.* **50,** 1019–1031 (2009).
32. Shpak, E. D., McAbee, J. M., Pillitteri, L. J. & Torii, K. U. Stomatal patterning and differentiation by synergistic interactions of receptor kinases. *Science* **309,** 290–293 (2005).
33. Berger, D. & Altmann, T. A subtilisin-like serine protease involved in the regulation of stomatal density and distribution in *Arabidopsis thaliana*. *Genes Dev.* **14,** 1119–1131 (2000).
34. Dong, J., MacAlister, C. A. & Bergmann, D. C. BASL controls asymmetric cell division in *Arabidopsis*. *Cell* **137,** 1320–1330 (2009).
35. Nadeau, J. A. & Sack, F. D. Control of stomatal distribution on the *Arabidopsis* leaf surface. *Science* **296,** 1697–1700 (2002).
36. Bhave, N. S. *et al.* TOO MANY MOUTHS promotes cell fate progression in stomatal development of *Arabidopsis* stems. *Planta* **229,** 357–367 (2009).
37. De Rybel, B. *et al.* Chemical inhibition of a subset of *Arabidopsis thaliana* GSK3-like kinases activates brassinosteroid signaling. *Chem. Biol.* **16,** 594–604 (2009).
38. Kim, T-W. *et al.* Brassinosteroid signal transduction from cell-surface receptor kinases to nuclear transcription factors. *Nat. Cell Biol.* **11,** 1254–1260 (2009).
39. Rozhon, W., Mayerhofer, J., Petutschnig, E., Fujioka, S. & Jonak, C. ASKθ, a group-III *Arabidopsis* GSK3, functions in the brassinosteroid signalling pathway. *Plant J.* **62,** 215–223 (2010).
40. Kim, T-W., Michniewicz, M., Bergmann, D. C. & Wang, Z-Y. Brassinosteroid regulates stomatal development by GSK3-mediated inhibition of a MAPK pathway. *Nature* **482,** 419–422 (2012).

DOI: 10.1038/ncb2471

METHODS

Plant material and growth conditions. *Arabidopsis thaliana* L. (Heyhn.) (Columbia ecotype, Col-0) was used as wild-type except where indicated. Plants were grown in plates with half-strength Murashige and Skoog (MS) medium without sugars, under a 16-h/8-h light–dark cycle at 22 °C. Plants grown for 21 days were transferred at day 8 to soil. Hormonal treatments were done on solid MS medium, except for the short treatments with BL, MG132 and cycloheximide. For protein or RNA extraction, seedlings were grown on a 20 µM nylon mesh placed on the agar to facilitate collection. Mutants used in this study were: *epf1* (ref. 29), *epf2* (refs 30,31), *er-105*, *erl1-2*, *erl2-1* (ref. 32), *sdd1* (ref. 33), *basl2* (ref. 34), *yda-5* (ref. 10), *tmm* (ref. 36), *spch-3* (ref. 5), *cpd* (ref. 17), *bri1-116* (ref. 18), *bin2-3*, *atsk22*, *atsk23* and its triple combination *bin2-3/atsk22/atsk23* (ref. 24), *bes1-D* (ref. 27) and *bzr1-D* (ref. 28). The *tmm* mutant was backcrossed into Col-0 to remove the *gl2* mutation[35]. *bin2-3* was obtained from a backcross of the triple *bin2-3/atsk22/atsk23* (ref. 24) into Col-0. DWF4OE (ref. 19), BRI1OE (ref. 18), *SPCHprom::SPCH–GFP* (ref. 2,5) and *SPCHprom::nGFP* (ref. 5) transgenic lines were described previously. BL, BRZ, MG132 and cycloheximide were purchased from Wako Pure Chemical Industries, Tokyo Chemical Industry and Merck, respectively.

Microscopy. For differential interference contrast microscopy, the epiderm[illegible] was cleared by subsequent incubations in ethanol, ethanol/10% acetic acid and ethanol/NaOH 1.25 M (1:1 v/v) at 60 °C for 2 h and overnight in lactic acid saturated in chloral hydrate. Counting of epidermal ce[illegible] stomata on days 4 and 8 was done in a ×200 field, and in two adjacent ×200 fields in the case of 21-day-old plants. All measurements in hypocotyls were performed at day 8. For electron microscopy, a TM-1000 scanning electron microscope (Hitachi) was used. Hypocotyls were observed directly, whereas moulds where created from abaxial epidermis of leaves or cotyledons using dental resin Genie VPS light body (Sultan Healthcare), from which a cast was created with nail polish and was used for imaging. Confocal microscopy was performed on abaxial cotyledon or hypocotyl epidermis from 2.5-day-old seedlings using LSM510 (Zeiss) or FluoView1000 (Olympus) inverted microscopes equipped with a water-corrected ×60 objective. Images were captured at 488 nm, 514 nm and 559 nm laser excitation and 500–530 nm and 570–670 nm long-pass emission for EGFP, RFP and propidium iodide staining (1 mg ml^{-1}). Fluorescent nuclei were counted in a ×200 field.

SPCH mutant versions and BIN2 reporter. *SPCH* complementary DNA was cloned into pDONR221 (Invitrogen). Mutagenesis of *SPCH* was performed with Pfu Ultra High Fidelity DNA Polymerase (Stratagene) and the primers listed in Supplementary Table S3. The *SPCH* promoter was amplified as described previously[5] and cloned into pDONRP4-P1 (Invitrogen). Wild-type and mutant versions of SPCH and the SPCH promoter were recombined into the Gateway vectors pK7m24GW or pK7m34GW (ref. 41) to generate translational fusions without and with GFP. The resulting constructs were transformed in the *spch-3* heterozygous mutant. Transformants were selected on antibiotic and genotyped for the *spch-3* background as described previously[5]. The SPCH promoter was recombined with pENL1-NR-L2 (ref. 41) and pENR2-R-L3 (ref. 41) vectors in pH7m34GW (ref. 41) to generate a transcriptional fusion with the nuclear localized RFP in tandem (*SPCHprom::nRFP*). The *BIN2* promoter was recombined into pXK7S∗NFm14GW (ref. 41) to generate a transcriptional fusion with the nuclear localized GFP (*BIN2prom::nGFP*). The *BIN2prom::nGFP* construct was transformed in wild-type Col-0 plants. Homozygous *BIN2p::nGFP*-expressing plants were subsequently transformed with the *SPCHprom::nRFP* construct.

Generation and purification of bacterially produced proteins. Wild-type and mutant *SPCH* were cloned into pGEX6P1. SPCHΔ93 was generated by PCR as described previously[2]. The resulting plasmids were transformed into *Escherichia coli* BL21Rosetta (DE3) cells. GST-tagged proteins were purified with glutathione–Sepharose 4B columns (GE-Healthcare) and, when specified, the GST tag was cleaved from GST–SPCH and GST–SPCHΔ93 with PreScission Protease (GE-Healthcare) according to the manufacturer's instructions.

SPCH immunoprecipitation. Proteins were extracted from 3 g of 2.5-day-old *pSPCH::SPCH:GFP*-expressing *Arabidopsis* seedlings[2,5] ground in ice-cold extraction buffer (50 mM Tris–HCl, at pH 7.5, 150 mM NaCl, 1% NP-40 and Complete protease inhibitor (Roche Diagnostics). The extracts were centrifuged at 13,000 r.p.m. at 4 °C for 20 min. Each sample was diluted to 2–4 mg ml^{-1} protein. A 1.5 ml volume of extracts was incubated with 20 µl of a 50% slurry of GFP-binding protein beads (GFP-Trap_A; Chromotek) at 4 °C for 4 h. After incubation, the beads were washed three times with 1 ml of washing buffer (20 mM Tris, at pH 7.5, 150 mM NaCl and 0.5% NP-40) and centrifuged at 500*g* to pellet the beads. The washed beads were mixed with 40 µl×2 SDS sample buffer and boiled for 5 min at 95 °C. Samples were separated by 12% SDS–PAGE and analysed by anti-GFP antibody (Living Colors A.v. Monoclonal Antibody (JL-8); Clontech) at 1:5,000 dilution.

***In vitro* kinase assay, mass spectrometry and phosphopeptide analysis.** *In vitro* kinase assays with recombinant proteins were carried out with 2 µCi[γ-^{32}P]ATP in 20 µl kinase buffer (20 mM HEPES, at pH 7.5, 15 mM $MgCl_2$ and 5 mM EGTA) for 30 min at room temperature. The reaction was stopped by the addition of 5 µl of ×4 SDS loading buffer. Proteins were resolved by 10% SDS–PAGE. After non-radioactive *in vitro* kinase assays, proteins were separated by SDS–PAGE, stained with a colloidal Coomassie staining solution and the excised bands were processed for phosphopeptides identification. Phosphopeptides were enriched by TiO_2 treatment[42,43] and identified by nano-LC–MS. The nano-HPLC system used was an UltiMate 3000 Dual Gradient HPLC system (Dionex), equipped with a Proxeonnanospray source (Proxeon), coupled to an LTQ VelosOrbitrap mass spectrometer (Thermo Fisher Scientific), operated in data-dependent mode using a full scan in the Orbitrap followed by MS/MS scans of the 12 most abundant ions in the linear ion trap. MS/MS spectra were acquired in the multistage activation mode, where subsequent activation was performed on fragment ions resulting from the neutral loss of −98, −49 or −32.6 m/z for phosphorylation site analysis. For peptide identification, all MS/MS spectra were searched using Mascot 2.2.04 (Matrix Science) against the Arabidopsis Information Resource protein sequence database. The carbamidomethylation on cysteine and the oxidation on methionine were set as fixed and as variable modification, respectively. Monoisotopic masses were searched within unrestricted protein masses for tryptic, chymotryptic and unspecific (subtilisin digest) peptides. Peptide and fragment mass tolerances were set to ±5 ppm and to ± 0.5 Da, respectively, whereas the maximal number of missed cleavages was set at 2. The result was filtered to 1% false discovery rate by means of the Percolator algorithm integrated into the Proteome Discoverer (1.3.0.339; Thermo Scientific). All phosphopeptides were also manually inspected. Accepted phosphopeptides, the related Mascot Ion Score and the precursor mass deviation are listed in Supplementary Table S1.

***In vivo* phosphopeptide identification.** Approximately 100 µl sterile *Arabidopsis* seeds expressing the *pSPCH::SPCH–GFP* construct[2,5] in the DWF4OE background were suspended in 100 ml liquid MS, vernalized at 4 °C for 2 days and transferred to light for 2.5 days at 22 °C under a 16-h/8-h light–dark cycle, shaking at 110 r.p.m. Seedlings were collected with an iron mesh and washed with water. The protein extract was prepared by grinding 5 g of seedlings with extraction buffer (50 mM Tris–HCl, at pH 7.5, 150 mM NaCl, 2% Triton X-100 and Complete protease inhibitor (Roche Diagnostics)) on ice. The extract was centrifuged at 13,000 r.p.m. at 4 °C for 30 min, then added with 100 µl of anti-GFP magnetic beads (Miltenyi Biotec) and incubated for 1 h on a rotating wheel at 4 °C. The beads were collected on a µMACS Separator (Miltenyi Biotec) and washed four times with 200 µl extraction buffer containing 0.1% Triton. The proteins were eluted from the beads with 65 µl of SDS loading buffer (Miltenyi Biotec) and processed as described before[44]. Briefly, a nano-LC set-up linked to a LTQ-Orbitrap XL (Thermo Electron) was used. Separated peptides were ionized through electrospray ionization. Full scan positive mode FTMS spectra were measured between m/z 380 and 1,400 in the Orbitrap at high resolution (60,000). CID MS/MS scans of the four most abundant multiply charged peaks in the FTMS scan were recorded in data-dependent mode in the linear trap (MS/MS threshold = 5,000). LCMS runs with all MS/MS spectra obtained were analysed with Bioworks 3.3.1 (Thermo Electron, Supplementary Table S2A). For quantification purposes, MaxQuant 1.2.2.5 (ref. 45) was employed with default settings for the Andromeda search engine[46] except that additional variable modifications were allowed for de-amidation of N and Q and phosphorylation of S, T and/or Y (Supplementary Table S1B). An *A. thaliana* database (http://www.uniprot.org) was used together with a contaminants database that contains sequences of common contaminants. The 'label-free quantification' as well as the 'match between runs' (set to 2 min) options were enabled. De-amidated peptides were included for protein quantification and all other quantification settings were kept in default mode. Phosphopeptide analyses after BL treatment were performed on *pSPCH::SPCH–GFP* (refs 2,5)-expressing DWF4OE[illegible]dlings. These seedlings still responded to a treatment of 50 nM BL with an inc[illegible]n the amount of SPCH–GFP protein comparable to that seen in the control. Seedlings were germinated in liquid MS containing either dimethylsulphoxide (DMSO) alone or with 50 nM BL. To increase the sensitivity of phosphopeptide detection, TiO_2 beads were used[47]. To accommodate for the lower amount of the SPCH protein present in the control DMSO-supplemented samples (Supplementary Fig. S4b), the amount of starting material after germination in BL was half of the amount present in the control sample. BL-treated samples and control samples were subsequently processed in parallel throughout the entire procedure (Supplementary Table S2B).

Quantitative RT-PCR. RNA was extracted from 2.5-day-old seedlings with the RNeasy mini kit (Qiagen). cDNA was generated with the iScript cDNA synthesis kit (Bio Rad). *SPCH* and *ACTIN* were amplified from 100 ng total RNA with the primers listed in Supplementary Table S3.

Statistical analysis. *P* values were calculated with a two-tailed Student *t*-test using Excel software.

41. Karimi, M., Bleys, A., Vanderhaeghen, R. & Hilson, P. Building blocks for plant gene assembly. *Plant Physiol.* **145,** 1183–1191 (2007).
42. Mazanek, M. *et al.* Titanium dioxide as a chemo-affinity solid phase in offline phosphopeptide chromatography prior to HPLC-MS/MS analysis. *Nat. Protoc.* **2,** 1059–1069 (2007).
43. Mazanek, M. *et al.* A new acid mix enhances phosphopeptide enrichment on titanium- and zirconium dioxide for mapping of phosphorylation sites on protein complexes. *J. Chromatogr. B* **878,** 515–524 (2010).
44. Karlova, R. *et al.* Identification of *in vitro* phosphorylation sites in the *Arabidopsis thaliana* somatic embryogenesis receptor-like kinases. *Proteomics* **9,** 368–379 (2009).
45. Cox, J. & Mann, M. MaxQuant enables high peptide identification rates, individualized p.p.b.-range mass accuracies and proteome-wide protein quantification. *Nat. Biotech.* **26,** 1367–1372 (2008).
46. Cox, J. *et al.* Andromeda: a peptide search engine integrated into the MaxQuant Environment. *J. Proteome Res.* **10,** 1794–1805 (2011).
47. Tingholm, T. E., Jørgensen, T. J., Jensen, O. N. & Larsen, M. R. Highly selective enrichment of phosphorylated peptides using titanium dioxide. *Nat. Protoc.* **1,** 1929–1935 (2006).

Page 1

Query 1:
Text amended to 'whereas the transition ... subsequent symmetric divisions' here. OK?

Query 2:
Please consider revising the long sentence 'The activity of ... (TMM).' to improve its readability (and remove the comma before 'that').

Query 3:
Can the text here be changed to '*bri1*-EMS-SUPPRESSOR1 (BES1; also known as BZR2), resulting' and the later two instances of 'BZR2/BES1' to 'BES1'? (According to style, solidas should not be used to mean 'also known as'.)

Query 4:
Can the text here be changed to '*dwarfism* (*cpd*; ref. 17), which is unable to synthesize BRs, and *bri1-116*, which is defective for BR perception'?

Page 2

Query 5:
'suggesting' changed to 'indicating' here, according to style. OK, or should, for example, 'is required' also be 'may be required'?

Page 3

Query 6:
'suggesting' changed to 'indicating' here, according to the query above. OK?

Query 7:
Please check that the intended meaning of the sentence 'Contrary to the ... Supplementary Fig. S2d).'has been retained after editing.

Page 5

Query 8:
Should the text here be 'reduction in phosphorylated Ser 171 and Ser 186 residues'?

Query 9:
'suggesting' changed to 'indicating' here, according to the query above. OK?

Page 6

Query 10:
'suggesting' changed to 'indicating' here, according to the query above. OK?

Query 11:
'suggests' changed to 'indicates' here, according to the query above. OK?

Query 12:
Should 'MAPK' be 'MAPK-' here?

Query 13:
Please provide affiliations for D. Bergmann, K. Torii, F. Sack, G. Vert, S. Mora-García, A. I. Caño-Delgado, H-Q. Yang and T. Kakimoto.

Page 7

Query 14:
Please confirm statement: 'The authors declare no competing financial interests.'

Page 8

Query 15:
'and' changed to comma before '*yda-5*' here. OK?

Query 16:
Four reagents are mentioned here, but three companies. Please check, and amend text to make clear which reagents are from which company.

Query 17:
'1.25 N' changed to '1.25 M' here, according to style. OK?

Query 18:
Text hyphenated to '21-day-old plants' here. OK?

Query 19:
Please provide *g* values or rotor details for the 'r.p.m.' value here and later (3 in total).

Query 20:
Text amended to 'and all other' here. OK?

General Queries

Query 21:
For the representation of gene symbols and genotypes we follow the standard scientific conventions and nomenclature found in databases such as HUGO for humans, MGI for mice or Flybase for Drosophila. Accordingly, many changes may have been made throughout the text and figures. Please check that we have interpreted each instance correctly.

Query 22:

Should ‘or seedlings (**a**,**d**...’ in the last sentence of figure 1’s caption be ‘or seedlings (**b**,**d**...’?

Query 23:

Please check that the intended meaning of figure 3d,e’s caption has been retained after editing.

Query 24:

As, according to style, mutations should be superscripted, can we make ‘S65A’, ‘S/T38-44A’, ‘S65A S/T38-44A’ and ‘Δ93’ superscript to ‘SPCH’ throughout? (So, for example, the text in figure 3d would become ‘SPCH$^{S65A\ S/T38-44A}$/*spch-3*’).

Query 25:

Can 2er, 3er and so on, in figure 5b (and L*er* in figure 2c and its caption), be defined? If so, please provide text to be added to the captions.